

## Measurements of Optical Phase Variations Using Interfering Multiphoton Ionization Processes

Ce Chen and D. S. Elliott

*School of Electrical Engineering, Purdue University, West Lafayette, Indiana 47907*

(Received 4 May 1990)

We have used interfering multiphoton ionization processes to measure changes in the relative phase between two optical laser beams. In this work, the phase variation is due to the  $\pi$  phase shift of a focused Gaussian beam as it propagates through the focal region. An array of linear collection electrodes is used to measure the multiphoton ionization rate as a function of the distance from the beam waist when two laser fields are resonant with an atomic transition, one through a linear process, the other through a three-photon process.

PACS numbers: 32.80.Rm

The phase of a laser field does not often produce a direct observable effect in its interaction with an atomic or molecular system. Recent observations<sup>1-10</sup> of competing optical interactions, however, are an important exception to this rule. In these experiments, the presence of optical fields at two or more different frequencies leads to the possibility of excitation of the atomic system by way of more than one process. For instance, an  $S \rightarrow P$  transition can be induced by a field at frequency  $\Delta E/\hbar$  through a linear interaction ( $\Delta E$  is the atomic transition energy), or through a three-photon process by a field at frequency  $\Delta E/3\hbar$ . In the presence of both fields, the two transition amplitudes will interfere, and the relative phase between the two optical fields becomes important. Potential applications in the area of laser-controlled chemistry have recently been proposed.<sup>11</sup>

This interference was first observed<sup>1-6</sup> indirectly through investigations of resonantly enhanced multiphoton ionization and multiphoton absorption. The surprising result was the reduction, and ultimate disappearance, of the multiphoton transition rate with increasing density of the atomic vapor. The explanation<sup>12-15</sup> for these observations rested with the interaction of the atomic vapor with *both* fields (one applied externally, the other generated internally through the nonlinear interaction) present in the vapor. It has been shown theoretically<sup>12-16</sup> that in a dissipative system, the relative phase of the two fields tends to become locked such that the interfering processes are  $180^\circ$  out of phase. This destructive interference between the transition amplitudes can lead to complete suppression of the absorption of both optical fields.

Recent experiments<sup>10</sup> have been performed in which the generation of harmonic fields and the photoionization processes have been spatially separated. This allows for the control of the interference in a way not possible in the experiments performed in a single vapor cell. The experiment was performed using the  $6s\ ^1S_0 \rightarrow 6p\ ^1P_1$  transition in atomic mercury. A pulsed tunable dye laser was tuned to 554 nm, corresponding to a frequency slightly to the blue of one-third the atomic transition fre-

quency. Third-harmonic radiation of the laser fundamental was produced in a high-density mercury vapor before the two collinear beams were focused into a low-density mercury cell in which the multiphoton ionization rate was measured. The relative phase between the two fields was varied by varying the density of a dispersive gas (argon) in a cell positioned between the harmonic-generation cell and the ionization cell. A 6-7-Torr change in the argon pressure produced a  $2\pi$  phase shift in the two transition amplitudes, resulting in a complete cycle in the modulation of the ionization probability.

In the present work, we apply these principles to a direct observation of the  $\pi$  phase shift of a focused Gaussian beam as the beam travels through the focal region. This work demonstrates the potential for measuring the phase variation resulting from a variety of effects such as parametric interactions or intensity-dependent refractive index of a nonlinear medium. The interference was observed in an experimental system very similar to what was reported previously.<sup>10</sup> Laser radiation consisting of an intense component of wavelength 554 nm (4-mJ pulse energy, 15-nsec pulse duration) and a weak component of wavelength 185 nm (the third harmonic of the first component) was focused into a vapor cell containing atomic mercury. The focal region was approximately centered between a ground plane and a set of eight biased collection electrodes. A schematic diagram of the experimental cell is shown in Fig. 1. Each electrode was constructed from a 1.27-mm-diam stainless-steel rod. They were aligned transverse to the direction of propagation of the laser beam, side by side, in a plane parallel to the ground plane with a center-to-center spacing of 1.65 mm. Each electrode collected the photoelectrons generated in the region directly between it and the ground plane. (The spatial resolution of the detector was limited by the spacing between electrodes, with a smaller contribution from the trajectory of the free electrons in the collection field.) The total charges detected by each of the electrodes were determined concurrently by an eight-channel gated integrator, and recorded using a laboratory personal computer. In this way we were

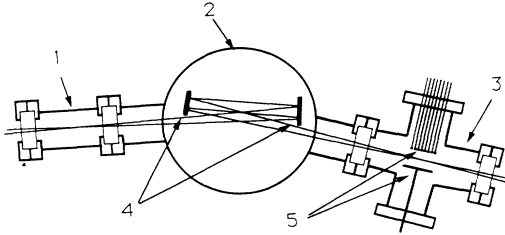


FIG. 1. Schematic diagram of the experimental cell. Chamber 1 contains mercury at a high density ( $\sim 100$  mTorr), 2 contains argon gas at a variable pressure (0–38 Torr), and 3 contains mercury at a low density ( $\sim 2$ –3 mTorr). In chamber 2 a pair of uv-enhanced aluminum-coated spherical mirrors (4) are used to refocus the laser beams diverging from chamber 1 into chamber 3. The ionization signals are measured using (5) a set of biased collection electrodes. The electrodes are parallel to each other, normal to the plane of the page. The bottom electrode is a grounded plane.

able to measure the number of photoelectrons generated in the laser beam at varying distances from the laser focus.

The  $z$  dependence of the ionization rate is easily calculated on the basis of weak-field interactions. This approximation is likely valid here because the laser is tuned off the resonance of the atomic transition. Dynamic Stark shifts do appear to be quite large for this transition, but we will ignore them in the present analysis. In

the presence of both fields we expected the net transition rate for the  $6s$ - $6p$  transition to be given by

$$W = \frac{2\pi}{h^2} |\mu E^{uv} e^{i\theta_1} + \mu^{(3)} (E^{vis} e^{i\theta_2})^3|^2 g(\Omega_{fg} - 3\omega), \quad (1)$$

where  $E^{uv}$  and  $E^{vis}$  are the electric-field amplitudes of the 185- and 554-nm beams, respectively,  $\mu$  and  $\mu^{(3)}$  are the transition moments for the linear and three-photon processes, respectively, and  $g(\Omega_{fg} - 3\omega)$  is a line-shape function. The phase of each field has been written explicitly in this expression, since when the two terms are summed, the phase difference will influence the process. When resonantly enhanced by the  $6s$ - $6p$  transition, the photoionization rate is expected to follow Eq. (1), with a possible additional multiplicative factor of  $(I^{vis})^2$  corresponding to the absorption of two additional visible photons required to ionize the atom. We will return to this point later. In either case, however, interference between the two excitation pathways is observable.

An additional factor which influences this interaction is due to the spatial dependence of the amplitudes and phases of the focused Gaussian beams used for making these observations. The relative magnitude of these two transition amplitudes, as well as their relative phase, vary through the focal region. We show this by including the spatial dependence of a focused Gaussian beam in the two fields in Eq. (1). This yields an atomic transition rate proportional to

$$W \propto \left| \frac{E_0^{uv} \mu e^{i\theta_1}}{[1 + (z/z_0)^2]^{1/2}} \exp\left[-\frac{3r^2}{w^2}\right] \exp\left[-i\left(k^{uv}z - \tan^{-1}\frac{z}{z_0}\right)\right] + \frac{(E_0^{vis} e^{i\theta_2})^3 \mu^{(3)}}{[1 + (z/z_0)^2]^{3/2}} \left\{ \exp\left[-\frac{r^2}{w^2}\right] \exp\left[-i\left(k^{vis}z - \tan^{-1}\frac{z}{z_0}\right)\right] \right\}^3 \right|^2, \quad (2)$$

where  $w(z)$  is the  $1/e^2$  intensity beam radius for the fundamental field,  $k$  is the propagation constant, and  $E_0$  is the field amplitude on the beam axis at the focus. Under our experimental conditions  $z_0 = \pi w^2(0)/\lambda$  is the same for the two beams, while the beam radius for the uv beam is  $1/\sqrt{3}$  that of the visible beam. Note the differences in the  $z$  dependence of the magnitudes of the transition amplitudes ( $[1 + (z/z_0)^2]^{-1/2}$  vs  $[1 + (z/z_0)^2]^{-3/2}$ ) and their phases ( $\tan^{-1}(z/z_0)$  vs  $3\tan^{-1}(z/z_0)$ ). The magnitude of the two processes can be matched at, at most, two locations symmetrically placed about the focus, and the phase of the two transition amplitudes varies by  $2\pi$  from  $z = -\infty$  to  $z = +\infty$ . Since each electrode was sensitive to all electrons generated at a certain distance  $z$  from the focus, we need to integrate Eq. (2) over the transverse dimensions. Finally, we set  $\Delta k = 3k^{vis} - k^{uv} = 0$ , valid at low mercury densities, and we generalize our result to that for an elliptical Gaussian beam, yielding an ionization rate proportional to

$$W(z) \propto 1 + \frac{M^2}{[1 + (z/z_{0x})^2][1 + (z/z_{0y})^2]} + \frac{2M}{[1 + (z/z_{0x})^2]^{1/2}[1 + (z/z_{0y})^2]^{1/2}} \cos\left[\phi_1 - 3\phi_2 - \tan^{-1}\left(\frac{z}{z_{0x}}\right) - \tan^{-1}\left(\frac{z}{z_{0y}}\right)\right], \quad (3)$$

where  $M = (E^{vis})^3 \mu^{(3)} / E^{uv} \mu$  represents the relative contribution of the two processes at the beam waist on axis.

Since the intensity of the laser varies through the focal region of the laser beam, and each electrode is sensitive to electrons generated in different regions, single-shot intensity-dependence measurements in a noninterfering case are attainable from the  $z$  dependence of the ionization signal. For example, if the five-photon ionization process is unsaturated, the ionization rate is proportional to  $I^5$ , leading to a  $z$  dependence of  $\{[1 + (z/z_{0x})^2][1 + (z/z_{0y})^2]\}^{-2}$ . On the other hand, if the final step ( $6p \rightarrow$  continuum) is saturated, so that the transition rate is proportional to  $I^3$ , then a  $z$  depen-

dence of  $\{[1+(z/z_{0x})^2][1+(z/z_{0y})^2]\}^{-1}$  would be observed. The data we have obtained clearly show that the latter is the case. Improvement of the technique is still necessary, since it appears that in our current configuration, the efficiency of the different electrodes varies, possibly due to electrode geometry. We expect to be able to report on this with more accuracy at a later date.

In spite of the need for refinement of the intensity-dependence measurements, the phase variation with  $z$ , as shown in Eq. (3), is very evident with the current electrode configuration. Figure 2 shows the ionization signal as a function of the argon pressure in the delay cell for a typical measurement set for six of the eight collection electrodes. Each data point represents the average of the ionization signal over 60–80 laser shots. Electrodes 1 and 8 were positioned sufficiently far from the focus of the laser so that only a weak ionization signal was detected, resulting in an insufficient signal-to-noise ratio. For each electrode data set, the average ionization rate has been subtracted leaving only the part which varies with the argon pressure. Each data set is seen to vary sinusoidally with the argon pressure with a period of around 6–7 Torr. This is in accord with the results reported previously. In the present data, a phase shift of the signal from one electrode to the next can be observed. This shift is due to the  $\tan^{-1}(z/z_0)$  terms in Eq. (3). By fitting a sinusoidal curve to each data set in Fig. 2, the relative phase shift of each electrode signal can be determined. These relative phases are shown in Fig. 3. Only about one-half of the total  $2\pi$  phase shift is visible since the ionization probability falls off rapidly for  $z/z_0$ . The error bars represent the estimated error in the phase, as determined from the scatter in the data shown

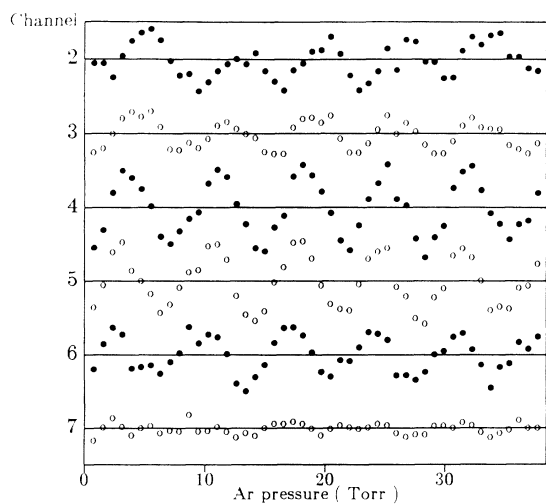


FIG. 2. Ionization signal as a function of argon pressure in the delay cell for individual electrodes. The average ionization signal has been subtracted from each data set, leaving only the part which varies with argon pressure.

in Fig. 2. The solid line represents the inverse tangent phase terms of Eq. (3). The values of  $z_{0x}$  and  $z_{0y}$  were derived from measurements of the beam radius of the nearly Gaussian beam before being focused into the first mercury vapor cell. The location of the focus ( $z=0$  point) was determined to within 1 mm from the  $z$  dependence of the ionization signal. The only adjustable parameter in Fig. 3, therefore, is a vertical offset of the data, since only a relative phase is determined through these measurements. Data points and calculated results (solid curves) for two different focusing conditions are shown in Fig. 3. In Fig. 3(a), a 20-cm focal-length lens was used, resulting in  $z_{0x}=3.65$  mm and  $z_{0y}=7.05$  mm. Figure 3(b) shows data for a 17-cm focal-length lens, yielding  $z_{0x}=2.64$  mm and  $z_{0y}=5.10$  mm. In each case, the data and calculations are in excellent agreement.

The depth of modulation of the interference signal, defined as the ratio of the amplitude of the sine wave to the average value, had a maximum value of 45% in this work. We have observed that the depth of modulation

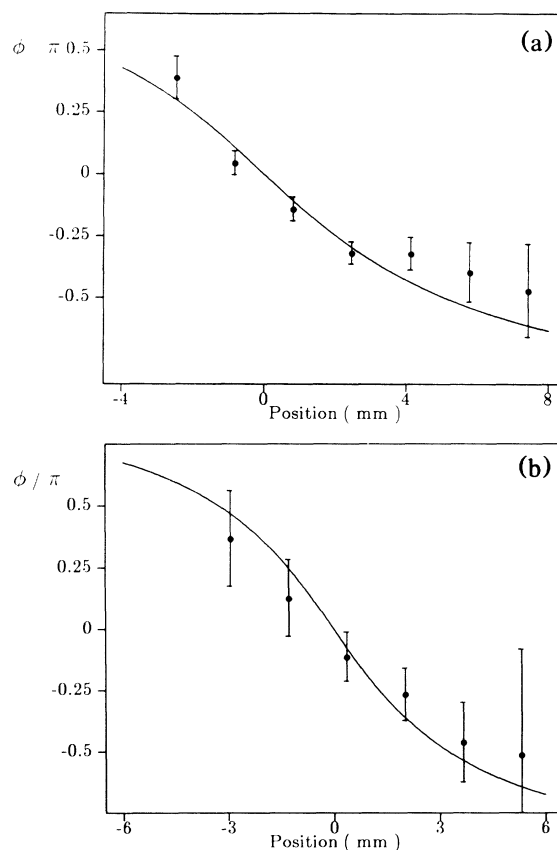


FIG. 3. The relative phase of the ionization signal as a function of  $z$ , the distance from the laser beam focus. The data in (a) and (b) correspond to two different confocal parameters of the focused elliptical Gaussian beam. In (a),  $z_{0x}=3.65$  mm and  $z_{0y}=7.05$  mm, while in (b),  $z_{0x}=2.64$  mm and  $z_{0y}=5.10$  mm. The solid line represents a calculation of the phase variation based on Eq. (3).

decreases along the  $z$  axis. This may possibly be due to phase locking of the waves related to harmonic generation in the mercury. Other limitations of the depth of modulation are due to nonoptimal values of  $M$ , incomplete spatial overlap of the two laser beams (in the transverse and axial directions), and finite resolution of the electrode array.

In conclusion, we have demonstrated the capability for measuring variations in the phase between optical transition amplitudes<sup>1</sup> using multiphoton ionization processes and a multielectrode detection configuration. This technique has the potential to yield single-shot intensity-dependence measurements as well. Future investigations of this work will be directed toward this goal, as well as toward measurements of phase effects such as those resulting from parametric interactions and applications toward achieving control of molecular photodissociation through two-path coherent excitations.

Useful discussions and assistance by Yi-Yian Yin have been helpful in this work. This work was supported by the National Science Foundation, Grant No. ECS-8451259. Support from Purdue University in the form of a David Ross grant is also acknowledged.

---

<sup>1</sup>K. Aron and P. M. Johnson, *J. Chem. Phys.* **67**, 5099 (1977).

<sup>2</sup>F. H. M. Faisal, R. Wallenstein, and H. Zacharias, *Phys. Rev. Lett.* **39**, 1138 (1977).

<sup>3</sup>R. N. Compton, J. C. Miller, and A. E. Carter, *Chem. Phys. Lett.* **71**, 87 (1980); J. C. Miller, R. N. Compton, M. G. Payne, and W. R. Garrett, *Phys. Rev. Lett.* **45**, 114 (1980); J. C. Miller and R. N. Compton, *Phys. Rev. A* **25**, 2056 (1982); M. G. Payne, W. R. Garrett, and W. R. Ferrell, *Phys. Rev. A* **34**, 1143 (1986); W. R. Garrett, W. R. Ferrell, M. G. Payne,

and J. C. Miller, *Phys. Rev. A* **34**, 1165 (1986).

<sup>4</sup>J. H. Glowina and R. K. Sander, *Appl. Phys. Lett.* **40**, 648 (1982); Y. I. Geller and A. V. Shvabouskas, *Opt. Spektrosk.* **53**, 385 (1982) [*Opt. Spectrosc. (U.S.S.R.)* **53**, 227 (1982)]; S. A. Bakhranov, I. Kirin, P. K. Khabibullaev, and N. S. Shaabdurakhmanova, *Kvantovaya Elektron. (Moscow)* **9**, 2386 (1982) [*Sov. J. Quantum Electron.* **12**, 1557 (1982)].

<sup>5</sup>D. Normand, J. Morellec, and J. Reif, *J. Phys. B* **16**, L277 (1983).

<sup>6</sup>J. H. Glowina and R. K. Sandner, *Phys. Rev. Lett.* **49**, 21 (1986).

<sup>7</sup>M. S. Malcuit, D. J. Gauthier, and R. W. Boyd, *Phys. Rev. Lett.* **55**, 1086 (1985); R. W. Boyd, M. S. Malcuit, D. J. Gauthier, and K. Rzazewski, *Phys. Rev. A* **35**, 1648 (1987).

<sup>8</sup>S. J. Bajic, R. N. Compton, J. A. D. Stockdale, and D. D. Knowalow, *J. Chem. Phys.* **89**, 7056 (1988).

<sup>9</sup>A. V. Smith (private communication).

<sup>10</sup>Ce Chen, Yi-Yian Yin, and D. S. Elliott, *Phys. Rev. Lett.* **64**, 507 (1990).

<sup>11</sup>M. Shapiro, J. W. Hepburn, and P. Brumer, *Chem. Phys. Lett.* **149**, 451 (1988); C. K. Chan, P. Brumer, and M. Shapiro, *Phys. Rev. Lett.* **64**, 3199 (1990).

<sup>12</sup>E. A. Manykin and A. M. Afanas'ev, *Zh. Eksp. Teor. Phys.* **48**, 931 (1965); **52**, 1246 (1967) [*Sov. Phys. JETP* **21**, 619 (1965); **25**, 828 (1967)].

<sup>13</sup>G. L. Gurevich and Yu. G. Khronopulo, *Zh. Eksp. Teor. Phys.* **51**, 1499 (1966) [*Sov. Phys. JETP* **24**, 1012 (1967)].

<sup>14</sup>M. G. Payne, W. R. Garrett, and H. C. Baker, *Chem. Phys. Lett.* **75**, 468 (1980); M. G. Payne and W. R. Garrett, *Phys. Rev. A* **26**, 356 (1982); **28**, 3409 (1983).

<sup>15</sup>D. J. Jackson and J. J. Wynne, *Phys. Rev. Lett.* **49**, 543 (1982); D. J. Jackson, J. J. Wynne, and P. H. Kes, *Phys. Rev. A* **28**, 781 (1983); J. J. Wynne, *Phys. Rev. Lett.* **52**, 751 (1984); in *Proceedings of the Fourth International Conference on Multiphoton Processes, Boulder, Colorado, 1987*, edited by S. J. Smith and P. L. Knight (Cambridge Univ. Press, Cambridge, 1987), p. 318.

<sup>16</sup>M. Poirier, *Phys. Rev. A* **27**, 934 (1983).